



Non-catalytic hydroamination of alkenes: a computational study

Sanyasi Sitha*, Linda L. Jewell

School of Chemical and Metallurgical Engineering, University of the Witwatersrand, Private Bag 3, Wits 2050, Johannesburg, South Africa

ARTICLE INFO

Article history:

Received 16 October 2009

Received in revised form 25 January 2010

Accepted 15 February 2010

Available online 18 February 2010

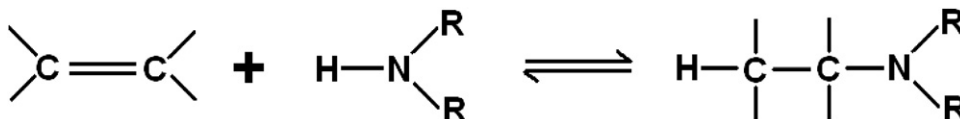
ABSTRACT

The detailed reaction profiles of the neutral–neutral as well as the cation–neutral direct hydroamination reactions between ethylene and ammonia are analyzed using MP2 (Full)/6-31++G(2df,2p) and B3LYP/6-31++G(2df,2p) methodologies. Analysis shows that both neutral–neutral, as well as the cation–neutral reactions are exothermic and the latter is >100 kJ/mol more exothermic than the former. Calculations show that a very large barrier height (>200 kJ/mol), and very large negative reaction entropy prevent the neutral–neutral reaction from proceeding in the forward direction. Analysis of the cation–neutral reaction, which is barrierless (the transition state is more stable than the reactants) and highly exothermic, indicates that the direct hydroamination reaction is thermodynamically attainable via a cation–neutral reaction pathway without a catalyst. Our calculations also suggest that although the cation–neutral direct hydroamination reaction is very fast, the cation of either ethylene or ammonia goes through a structural relaxation process before reacting with the other neutral reactant.

© 2010 Elsevier Ltd. All rights reserved.

1. Introduction

The hydroamination of alkenes, which proceeds through the formal addition of an N–H bond across a carbon–carbon double bond (Scheme 1), is an elegant synthetic organic transformation, which offers an attractive route to numerous classes of organo-nitrogen molecules, such as alkylated amines, enamines or imines.^{1–14} The synchronous direct addition of ammonia to an alkene to produce the amine is of seemingly fundamental simplicity and is highly desirable from an industrial point of view, as several tons of amines are produced worldwide every year.^{1,2,5,8}



Scheme 1.

As can be seen from Scheme 1, direct hydroamination processes convert inexpensive and readily available starting materials into the desired products in a single reaction without any formation of side products, and therefore theoretically proceed with 100% atom efficiency.¹ Thus a direct hydroamination process might offer significant economic and environmental benefits compared to classical methods for the synthesis of amines. Thermodynamic

considerations indicate that this direct addition reaction is exothermic ($\Delta H_R = -52.7$ kJ/mol) and the free energy of the addition, ΔG_R is -14.7 kJ/mol.^{6,7} However, the reaction is hindered by a high activation barrier caused by repulsive intermolecular interactions between the π -cloud of the olefin and the lone pair of the NH_3 , which arise during the approach of the amine and alkene.^{1,2,7} Also, a [2+2] cycloaddition of N–H to the alkene would be an orbital symmetry-forbidden process, which is unfavorable because of the high-energy difference between $\pi(\text{C}=\text{C})$ and $\sigma(\text{N}-\text{H})$.² It is not possible to overcome the activation barrier simply by performing the hydroamination reaction at elevated temperature, as it is

associated with a large negative reaction entropy ($\Delta S_R = -127.5$ J/mol K), which will shift the equilibrium of the hydroamination reaction towards the starting materials with increasing temperature.^{1,2,4,7} Therefore catalytic procedures are indispensable for the hydroamination of olefins, and considerable effort has been made to develop organometallic based catalysts, which either activate the olefin or the ammonia, to make the reaction feasible [for a comprehensive review, see: Ref. 2].

In the recent work of Hamann et al., the traditional organometallic catalyst of the hydroamination reaction of $\text{CH}_2=\text{CH}_2$ with NH_3 was replaced with a low energy electron beam.¹⁵ They have

* Corresponding author.

E-mail address: sanyasi.sitha@wits.ac.za (S. Sitha).

shown that, in the first step, the electron beam ionizes one of the reactants, which then reacts with the other neutral reactant, in a favorable ion–molecule interaction: they have ionized each of the reactants in separate experiments, both of which resulted in the production of cationic ethyl amine.¹⁵ This experiment makes this atom economic and environmentally friendly hydroamination reaction feasible. This cation–neutral hydroamination reaction resembles the traditional catalytic hydroamination reaction. The first step in the catalytic hydroamination reaction is the activation of either ethylene or amine, where either of the reactants forms a co-ordination complex by donating its electrons and thus making itself partially positive and susceptible to nucleophilic attack.² Similarly in the cation–neutral reaction, activation of either of the reactants is done by the electron beam to generate cations and thus make them susceptible to nucleophilic attack. One major difference is that, in the catalytic process, the complex formed between the reactant and the metal complex is quite stable (so stable that the subsequent reaction with the other reagent sometimes does not occur), whereas in the cation–neutral process the generated cation is highly unstable.² Hamann et al. reported that cation–neutral hydroamination reactions are very fast.¹⁵ Thus for the simplest case, i.e., the addition of the NH₃ to CH₂=CH₂, it has been established that the direct addition is experimentally feasible, but little or almost no attention has been given to exploring this reaction theoretically. In this work, we have carried out a computational study to explore the complete reaction mechanism of the hydroamination reaction by considering this simplest case, namely the ethylene and ammonia system. Our goals in this study are twofold: (1) to explore the reaction path of the neutral–neutral hydroamination reaction including the energetics of the transition state, and (2) to investigate the two proposed cation–neutral hydroamination reaction pathways as described by Hamann et al.¹⁵ where one proceeds through the ionization of the ethylene and the other proceeds through the ionization of the ammonia.

2. Computational methods

All the calculations were carried out using MP2(Full)/6-31++G(2df,2p) and B3LYP/6-31++G(2df,2p) level of theories, implemented in the Gaussian 03 program package, at the default 298.15 K and 1 atm conditions.¹⁶ For the closed shell species, the RMP2 and RB3LYP methods, and for the open shell species, UMP2 and UB3LYP methods were employed during optimization. During the full MP2 calculations, all the electrons are taken into consideration. For both methods, Pople's basis set with double diffuse functions is used in the calculation, in addition to two sets of d-functions and one set of f-functions on the C- and N-atoms, and two sets of p-functions on the hydrogens. The true minima and the transition states are confirmed from analysis of their frequencies by ensuring that all frequencies were positive for the minimum, with only one imaginary frequency for the transition state. Since the reaction is reported to be very fast, for the cations we have carried out full minimizations (geometry relaxation) and also single point energy calculations with a unit positive charge, at the optimized geometries of their neutral counterparts. Localization of the transition states was carried out using the Berry optimization to a saddle point of order one (the keyword to call this procedure in Gaussian 03 is OPT=TS).¹⁶

Thermodynamic quantities like ΔH_R , ΔG_R , ΔS_R and the activation barriers (E^a and E^b are the activation energies for forward and reverse reactions) are calculated from the energies of the reactants, product and transition states, using the equations as shown below.

$$\Delta H_R = \Delta H_{\text{PRODUCT}} - \Delta H_{\text{REACTANTS}}$$

$$\Delta G_R = \Delta G_{\text{PRODUCT}} - \Delta G_{\text{REACTANTS}}$$

$$\Delta S_R = (\Delta H_R - \Delta G_R)/T$$

$$\Delta E_R = \Delta E_{\text{PRODUCT}} - \Delta E_{\text{REACTANTS}}$$

$$E^a = \Delta E_{\text{TS}} - \Delta E_{\text{REACTANTS}}$$

$$E^b = \Delta E_{\text{TS}} - \Delta E_{\text{PRODUCT}}$$

3. Results and discussion

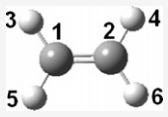
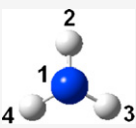
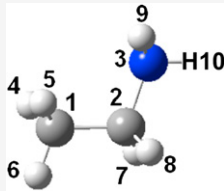
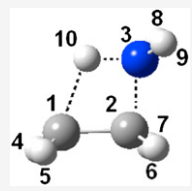
3.1. Neutral–neutral reaction

The two reactants in the neutral–neutral direct hydroamination reaction considered are ethylene (CH₂=CH₂) and ammonia (NH₃). Ethylene is in a fully planar configuration with *D*_{2h} symmetry and is in the singlet ¹A_g state. As can be seen from Table 1, the C–C distance is almost the same in the MP2 (1.333 Å) and B3LYP (1.331 Å) methods. Ammonia is C_{3v} symmetric and in the singlet ¹A₁ state; it adopts a pyramidal shape with the angle of pyramidality being 38.7° and 38.0°, determined using MP2 and B3LYP methods, respectively. Being symmetric, the dipole moment of the ethylene is zero, whereas the resultant dipole moment of the ammonia molecule is 1.70 D and 1.60 D, respectively, for MP2 and B3LYP methods and is unidirectional (negative z-axis). The product, ethyl amine (CH₃–CH₂–NH₂) was optimized with no symmetry restrictions and is in the ¹A state. The optimized N–C bond length (*R*_{2,3}) is 1.460 Å and 1.468 Å, the C–C–N bond angle (*A*_{3,2,1}) is 109.7° and 110.6°, and the nitrogen pyramidality (*D*_{2,9,10,3}) is 34.1° and 33.4°, respectively, using the MP2 and B3LYP methods. The dipole moment of the product is 1.39 D and 1.30 D, respectively, in the MP2 and B3LYP methods, and the major dipole component is along the positive z-axis. The dipole moment of the product is reduced compared to the dipole moment of the reactant (dipole moment of the NH₃).

The transition state in the reaction path was also optimized using MP2 and B3LYP methodologies. The observed transition state is C_s symmetric and is characterized by one imaginary frequency (–1144.9 cm^{–1} in MP2 and –1264.3 cm^{–1} in B3LYP methods). The dipole moment values are 5.08 D and 4.06 D, respectively, for MP2 and B3LYP methodologies, and the major dipole component is in the x-direction. Analysis of the key structural parameters shows that the C=C bond (*R*_{1,2}) is a little elongated (1.484 Å in MP2 and 1.492 Å in B3LYP methods) compared to the reactant ethylene, and also that one of the N–H bonds (*R*_{3,10}) is elongated (1.139 Å and 1.159 Å in MP2 and B3LYP methodologies, respectively) compared to the reactant ammonia (1.011 Å and 1.015 Å in MP2 and B3LYP methodologies). The N–H bond is directly above the C=C bond in the transition state structure, so that the C₁–H (H of N–H) distance (*R*_{1,10} where the H is bound to N via an elongated bond) is 1.741 Å and 1.724 Å, respectively, in MP2 and B3LYP methods and the C₂–N distance (*R*_{2,3}) is 1.563 Å and 1.588 Å in MP2 and B3LYP methods, respectively. Comparing the *R*_{1,2} distance of the TS with the product it can be seen that the product shows a distance, that is characteristic of a single bond, and the TS has a bond length, that is in between a single and a double bond. Comparing the *R*_{2,3} distance of the TS with that of the product shows that the TS distance is slightly elongated compared to the equilibrium product bond distance.

To account for the nature of interaction, the orbital interaction diagram for the reactants, product and the transition state obtained from the B3LYP population analysis is shown in Figure 1. Transition state structural analysis reveals that the nature of interaction is between the C=C of the ethylene and the N–H bond and in the light of this, the frontier molecular orbital analysis of the reactants shows that the interaction is possibly between the HOMO of the ethylene and the HOMO–1 of the ammonia. The molecular orbital energy of the HOMO of ethylene is –7.6 eV and that of the HOMO–1

Table 1
Key structural parameters, dipole moments and thermodynamic factors for reactants, product and the TS of the neutral–neutral hydroamination reaction are calculated using the MP2 and B3LYP methods. Structural parameters R_{pq} are represented in Å, A_{pqr} and D_{pqrs} are represented in degrees, dipole moments are in Debye, thermodynamic factors ΔE , ΔH and ΔG are represented in kJ/mol and absolute energies in Hartree. All the energy values corrected for ZPE

Neutral species	MP2			B3LYP		
	Key structural parameters	Dipole	Thermodynamic factors and absolute energy	Key structural parameters	Dipole	Thermodynamic factors and absolute energy
Ethylene 	$R_{1,2}=1.333$ $R_{1,3}=1.081$ $A_{3,1,5}=117.0$ $A_{3,2,1}=121.5$ $D_{3,1,2,4}=0.0$	0.00	$\Delta E=0.0$ $\Delta H=0.0$ $\Delta G=0.0$ $E_{[\text{CH}_2=\text{CH}_2]}=-78.33,1773$	$R_{1,2}=1.331$ $R_{1,3}=1.086$ $A_{3,1,5}=116.5$ $A_{3,2,1}=121.8$ $D_{3,1,2,4}=0.0$	0.00	$\Delta E=0.0$ $\Delta H=0.0$ $\Delta G=0.0$ $E_{[\text{CH}_2=\text{CH}_2]}=-78.552,044$
Ammonia 	$R_{1,2}=1.011$ $A_{2,1,3}=107.1$ $D_{4,3,2,1}=38.7$	1.70	$E_{[\text{NH}_3]}=-56.400,856$	$R_{1,2}=1.015$ $A_{2,1,3}=107.5$ $D_{4,3,2,1}=38.0$	1.60	$E_{[\text{NH}_3]}=-56.536,249$
Ethyl Amine 	$R_{1,2}=1.516$ $R_{1,3}=2.432$ $R_{2,3}=1.460$ $A_{3,2,1}=109.7$ $D_{2,9,10,3}=34.1$	1.39	$\Delta E=-69.7$ $\Delta H=-76.2$ $\Delta G=-34.4$ $E_{[\text{Product}]}=-134.759,165$	$R_{1,2}=1.527$ $R_{1,3}=2.462$ $R_{2,3}=1.468$ $A_{3,2,1}=110.6$ $D_{2,9,10,3}=33.4$	1.30	$\Delta E=-45.1$ $\Delta H=-51.4$ $\Delta G=-10.0$ $E_{[\text{Product}]}=-135.105,454$
TS 	$R_{1,2}=1.484$ $R_{1,3}=2.343$ $R_{3,10}=1.139$ $R_{1,10}=1.741$ $R_{2,3}=1.563$ $A_{3,2,1}=100.5$ $A_{10,3,2}=83.8$ $A_{1,10,3}=107.1$ $A_{2,1,10}=68.7$ $D_{1,2,3,10}=0.0$	5.08	$\Delta E=216.3$ $\Delta H=209.9$ $\Delta G=250.7$ $E_{[\text{TS}]}=-134.650,248$	$R_{1,2}=1.492$ $R_{1,3}=2.359$ $R_{3,10}=1.159$ $R_{1,10}=1.724$ $R_{2,3}=1.588$ $A_{3,2,1}=99.9$ $A_{10,3,2}=82.5$ $A_{1,10,3}=108.2$ $A_{2,1,10}=69.4$ $D_{1,2,3,10}=0.0$	4.06	$\Delta E=228.9$ $\Delta H=222.4$ $\Delta G=263.8$ $E_{[\text{TS}]}=-135.001126$

of the ammonia is -12.7 eV. The energy difference of 5.1 eV gives a clear indication that the interaction is not favourable from an energetic point of view. This is in good agreement with the earlier reports where it is indicated that the reaction is unfavourable due to the high-energy difference between $\pi(\text{C}=\text{C})$ and $\sigma(\text{N}-\text{H})$ bonds.^{1,2}

Now, analyzing the interaction, which is a two orbitals-four electron type of interaction, it is well known that the interaction will be repulsive as the resultant bonding and antibonding orbitals will both be filled.¹⁷ Also, in the resultant orbitals, the stabilization effect will be small compared to the destabilization effect.¹⁷ Our calculation indicates similar behavior, where the destabilization of the HOMO of the transition state with respect to the HOMO of the ethylene (3.1 eV) is greater than the stabilization of the HOMO-5 of the transition state with respect to the HOMO-1 of ammonia (1.8 eV). Our analysis shows that, although a $[2+2]$ cycloaddition of N-H to the alkene is an orbital symmetry-forbidden process,^{1,2} the reaction proceeds through this forbidden reaction pathway and thus raises the energy of the transition state to an exceptionally large value.

The potential energy surface of the neutral–neutral direct hydroamination reaction path is shown in Figure 2. All the energies are represented in kJ/mol and are zero point energy (ZPE) corrected. From the potential energy surface, it can be seen that, the reaction goes through a high energy barrier of 216.3 kJ/mol

and 228.9 kJ/mol, respectively, for MP2 and B3LYP methods with respect to the reactants $\text{CH}_2=\text{CH}_2+\text{NH}_3$ (the barrier height for the reverse reaction is 286.0 kJ/mol and 274.0 kJ/mol in MP2 and B3LYP methodologies, respectively). Comparing energies of the reactants and product it can be seen that the reaction is exothermic (-69.7 kJ/mol and -45.1 kJ/mol, respectively, for MP2 and B3LYP methods, respectively). In some earlier works, it was reported that the reaction indeed proceeds through a high energy barrier and is exothermic in nature, but no numerical value was given for the exact barrier height.^{1,2,7} Our calculation agrees with these reports showing a very large energy barrier in this reaction path and that the reaction is exothermic. Also, from Table 1, it can be seen that the reported experimental ΔH , ΔG and ΔS , -52.7 kJ/mol, -14.7 kJ/mol and -127.5 J/mol K, respectively, are in agreement with our calculated values (ΔH , -76.2 kJ/mol and -51.4 kJ/mol, ΔG , -34.4 kJ/mol and -10.0 kJ/mol and ΔS , -140.2 J/mol K and -138.9 J/mol K for MP2 and B3LYP methods, respectively).^{6,7} Comparing our calculated values with the reported experimental results, it can be seen that the B3LYP results are in very good agreement with the experimental values, whereas the MP2 results are slightly higher in value, but nevertheless agree in terms of the trend. Lastly, our calculation confirms that the very large activation barrier and the large negative reaction entropy are the key factors responsible for forbidding the reaction from proceeding in the forward direction.

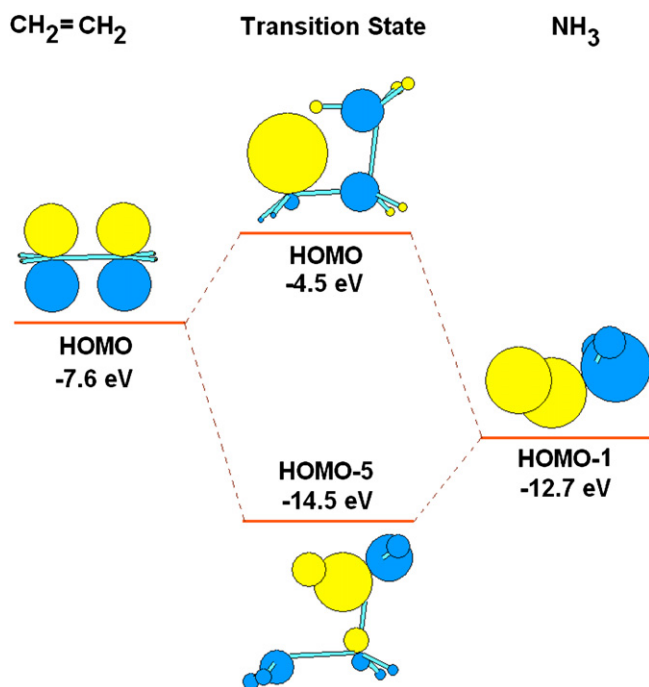


Figure 1. Molecular orbital interaction diagram for the neutral–neutral hydroamination reaction. Molecular orbital pictures are obtained from the population analysis of the B3LYP/6-31++C(2df,2p) optimized geometries. Orbital energy levels are not to scale.

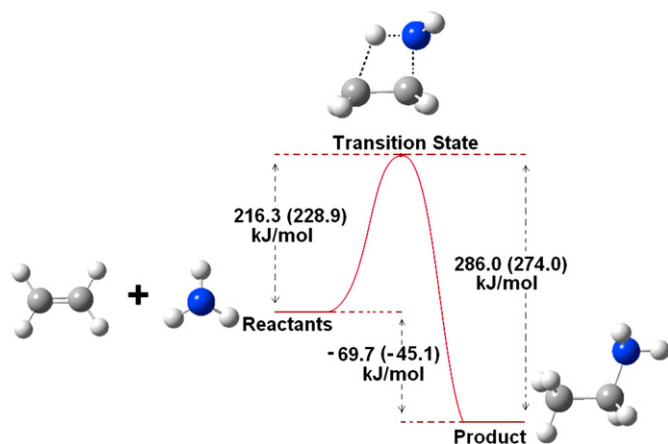


Figure 2. Potential energy surface of the neutral–neutral hydroamination reaction. The ZPE corrected energy values are represented in kJ/mol for MP2 and B3LYP methodologies (B3LYP values are given in brackets).

3.2. Cation–neutral reaction

The recent experimental work of Hamman et al. is a positive step towards achieving stoichiometric and environmentally friendly direct hydroamination.¹⁵ In their approach they have adopted cation–neutral hydroamination without the traditional catalysts. The cation–neutral hydroamination reaction proceeds through the reaction of the cationic form of either NH_3 or $\text{CH}_2=\text{CH}_2$ with neutral $\text{CH}_2=\text{CH}_2$ or NH_3 , respectively, and leads to two reaction pathways as proposed by Hamann et al.¹⁵ In this work we have carried out a computational study to estimate the energetics of those two proposed reaction pathways for the cation–neutral hydroamination reaction. The results are compared to the neutral–neutral hydroamination reaction (Section 3.1). As discussed in the report by Hamann et al.,¹⁵ in the first step a cation is produced by

the ionization of either one of the two reactants by a low energy electron beam. Hamann et al. reported that cation–neutral hydroamination reactions are very fast.¹⁵ As a result we have considered two possible starting points for the calculation of the reaction, namely: that the cation will immediately react with the other neutral reactant without any structural relaxation, or that the cation undergoes structural relaxation and then reacts with the other neutral reactant. In the former case the cation will have the same geometry as its neutral counterpart and in the latter case the cation will have a geometry, that is different from its neutral counterpart.

3.2.1. Cations of ammonia and ethylene. Radical cations of either ammonia or ethylene can be calculated in two different ways. First, without any structural relaxation, single point energies can be calculated for the cation of the ammonia and ethylene at their corresponding neutral optimized geometries. In this way the cations of ammonia and ethylene have the same geometry as that of their neutral counterparts, but because of the positive charge, properties (like dipole moments and charges) will be expected to change. Second, the cations of ammonia and the ethylene can be fully optimized and the relaxed geometries thus obtained are completely different from neutral ammonia and ethylene, respectively. Combined with the structural changes and positive charges, these cations also show different properties compared to their neutral counterparts. As expected, the dipole moments of the unrelaxed geometry of the cation of the ammonia are 1.11 D and 1.09 D, respectively, in MP2 and B3LYP methods, and the unrelaxed geometry of the cation of ethylene has a zero dipole moment value in both the methods. Cationic ammonia with unrelaxed geometry shows a reduction in dipole moment value in both methods compared to its neutral counterpart, and cationic ethylene with unrelaxed geometry shows a zero dipole moment due to its planar structure.

The fully minimized key structural parameters of the cations of ethylene and ammonia along with their dipole moment values for MP2 and B3LYP methods are shown in Table 2. Note that

Table 2

Key structural parameters and dipole moments for the fully minimized cations of the reactants, product and the TS of the cation–neutral hydroamination reaction are calculated using the MP2 and B3LYP methods. Structural parameters R_{pq} are represented in Å, A_{pqr} and D_{pqrs} are represented in degrees and dipole moments are in Debye. As the number of atoms in cation and neutral species is same, hence refer to Table 1 for atom numbering of the reactants, product and TS

Cationic Species	MP2	Dipole	B3LYP	Dipole
	Key structural parameters		Key structural parameters	
[Ethylene] ⁺	$R_{1,2}=1.409$ $R_{1,3}=1.084$ $A_{3,1,5}=118.9$ $A_{3,2,1}=120.5$ $D_{3,1,2,4}=12.0$	0.0	$R_{1,2}=1.394$ $R_{1,3}=1.091$ $A_{3,1,5}=117.7$ $A_{3,2,1}=121.1$ $D_{3,1,2,4}=28.2$	0.0
[Ammonia] ⁺	$R_{1,2}=1.019$ $A_{2,1,3}=120.0$ $D_{4,3,2,1}=0.0$	0.0	$R_{1,2}=1.026$ $A_{2,1,3}=120.0$ $D_{4,3,2,1}=0.0$	0.0
[Ethyl Amine] ⁺	$R_{1,2}=1.511$ $R_{1,3}=2.446$ $R_{2,3}=1.420$ $A_{3,2,1}=113.1$ $D_{2,9,10,3}=1.6$	3.82	$R_{1,2}=1.516$ $R_{1,3}=2.478$ $R_{2,3}=1.416$ $A_{3,2,1}=115.3$ $D_{2,9,10,3}=0.0$	3.15
[TS] ⁺	$R_{1,2}=1.513$ $R_{1,3}=2.123$ $R_{3,10}=1.403$ $R_{1,10}=1.313$ $R_{2,3}=1.487$ $A_{3,2,1}=90.1$ $A_{10,3,2}=82.6$ $A_{1,10,3}=102.7$ $A_{2,1,10}=84.6$ $D_{1,2,3,10}=0.0$	1.83	$R_{1,2}=1.521$ $R_{1,3}=2.167$ $R_{3,10}=1.396$ $R_{1,10}=1.364$ $R_{2,3}=1.507$ $A_{3,2,1}=91.4$ $A_{10,3,2}=82.3$ $A_{1,10,3}=103.4$ $A_{2,1,10}=82.9$ $D_{1,2,3,10}=0.0$	1.66

there was negligible spin contamination found during optimization. The fully minimized geometry of the ethylene cation shows a non planar D_2 symmetric structural arrangement. The C–C bond length ($R_{1,2}$) is 1.409 Å in the MP2 method and 1.394 Å in the B3LYP method compared to the experimental value of 1.405 Å, which shows that the MP2 result is very close to the experimental value.²³ Comparing the other parameters R_{C-H} , $\angle H-C-H$ and the torsion angle from the experimental studies (R_{C-H} , $\angle H-C-H$ and $\angle H-C-C-H$ torsion angle values are 1.091 Å, 117.8° and 25.0°, respectively) with that of the calculated MP2 (R_{C-H} , $\angle H-C-H$ and $\angle H-C-C-H$ torsion angle values are 1.084 Å, 118.9° and 12.0°, respectively) and B3LYP (R_{C-H} , $\angle H-C-H$ and $\angle H-C-C-H$ torsion angle values are 1.091 Å, 117.7° and 28.2°, respectively) results, it can be seen that the B3LYP results are closer to the experimental values.^{23–26} Although both the MP2 and B3LYP methods are in good agreement with the experimental results, there is a large discrepancy between the torsion angle predicted by the MP2 method and the experimental value. The fully minimized geometry of the ammonia cation shows a planar structural arrangement with D_{3h} symmetry, which is in good agreement with the earlier computational and experimental works.^{18–22} Compared to the experimental N–H bond length of 1.014 Å, MP2 results are in very good agreement; whereas the B3LYP method predicts a slightly longer bond length (N–H bond length, $R_{1,2}$ is 1.019 Å in the MP2 method and 1.026 Å in the B3LYP method).¹⁹ Nevertheless both MP2 and B3LYP results are very close to the experimental value.

3.2.2. Cation of ethyl amine. Cationic ethyl amine, $[CH_3-CH_2-NH_2]^+$ was fully optimized with no symmetry restrictions and is in the 2A state. The minimized key structural parameters and the dipole moments of the cationic ethyl amine calculated using MP2 and B3LYP methods are shown in Table 2. Note that there was negligible spin contamination found during optimization. Analyzing the geometry of the cationic ethyl amine, it can be seen that it is structurally similar to that of the neutral ethyl amine. The optimized N–C bond length ($R_{2,3}$) is 1.420 Å and 1.416 Å, the C–C–N bond angle ($A_{3,2,1}$) is 113.1° and 115.3°, respectively in the MP2 and B3LYP methods and also the pyramidality of the $-NH_2$ nitrogen (see the $D_{2,9,10,3}$ values) is completely lost in both of the methods. It can be seen that the $-NH_2$, which was pyramidal in the neutral case became almost planar in the cation of ethyl amine and this is the only major structural change between the cation and the neutral amine. The molecule has dipole moment values of 3.82 D and 3.15 D, respectively in MP2 and B3LYP methods, and the major component is along the negative x -axis. Comparing the total dipole moments of the cationic ethyl amine with that of the neutral ethyl amine, an increase in the value is seen in both MP2 and B3LYP methodologies, and this is expected for an unsymmetric charged species. Both the neutral ethylene and the cationic form have zero dipole moments. If one compares the dipole moment of the cationic ethyl amine with that of the reactant, ammonia, it can be seen that the dipole moment of the cationic ethyl amine is larger than either the neutral or the cationic form of the ammonia. The neutral and cation single point calculated dipole moment values for the neutral geometry of the ammonia are in a similar range, whereas the fully optimized cation of the ammonia has a zero dipole moment due to its planar structure. Analysis of the spin densities of the cationic ethyl amine shows that almost the entire spin density resides on the N-atom. In the complete reaction profile of the cation–neutral hydroamination reaction, the cationic ethyl amine will further undergo electron recombination and geometry relaxation processes to give the final product, ethyl amine (neutral).¹⁵ As this work deals with the mechanistic study of the cation–neutral hydroamination reaction, energetics of this latter process are not discussed here. However,

we have compared the geometry of the cation with the neutral ethyl amine.

3.2.3. Transition state of cation–neutral reaction. Our search for a transition state in the cation–neutral hydroamination reaction potential energy surface resulted in a structure, which has a similar arrangement to that of the transition state, that is, obtained in the neutral–neutral hydroamination reaction. Frequency analysis shows that there is only one imaginary frequency (-1771.5 cm^{-1} and -1728.4 cm^{-1} in MP2 and B3LYP methods) and the complex can be considered as a transition state. Analyzing and comparing the structural arrangement of this transition state of the cation–neutral reaction with that of the transition state of the neutral–neutral hydroamination reaction, it can be seen that in both cases the addition of the N–H of ammonia occurs over the C=C of the ethylene and both are C_s symmetric in nature. The dipole moment values for this transition state like complex are 1.83 D and 1.66 D from MP2 and B3LYP methods and are larger than the dipole moment values of the transition state of the neutral–neutral reaction. Analysis of the dipole vector components shows that the major dipole component is in the x -direction and is similar to that of the direction in the transition state of the neutral–neutral reaction. For a better understanding of the geometry of this transition state, a few of its key structural parameters are compared with the reactants as well as the transition state of the neutral–neutral reaction (Table 2). The C=C bond length ($R_{1,2}$) of the TS for the cation–neutral reaction is 1.513 Å and 1.521 Å, respectively for MP2 and B3LYP methods, and is a little elongated compared to the C=C bond length of either the neutral or the cationic form of ethylene given by the respective methodologies. Also it is elongated compared to the C=C bond length in the transition state of the neutral–neutral reaction, in the respective methodologies. The N–H segment ($R_{3,10}$), which is directly above the C=C segment in the TS has a distance of 1.403 Å and 1.396 Å in the MP2 and B3LYP methods and is enlarged to a great extent compared to the N–H bond length of the neutral and cationic form of ammonia and also the N–H bond length in the transition state of the neutral–neutral reaction, in the respective methodologies. Interestingly, comparing the N–H distance of the transition state of the cation–neutral reaction and transition state of the neutral–neutral reaction, the latter suggests a bonded state of the 'H' to the 'N' and the former indicates that the H is completely detached from the N. Further analysis shows that the C_1 –H (H of N–H) distance ($R_{1,10}$) for the complex is of 1.313 Å and 1.364 Å, respectively and the C_2 –N distance ($R_{2,3}$) is of 1.487 Å and 1.507 Å in MP2 and B3LYP methods, respectively. Comparing these data with that of the transition state of the neutral–neutral reaction, it can be seen that the C_2 –N bond in this complex is little shorter and the C_1 –H bond is much shorter in the respective methodologies. This gives a clear indication that the interaction in the complex of the cation–neutral reaction is stronger than that of the interaction in the transition state of the neutral–neutral reaction. This strong interaction, which arises due to a favourable ion–molecule type of interaction might be responsible for stabilizing the TS, placing it below the reactants in the potential energy surface and so eliminating the energy barrier of the reaction. Comparing the TS with the cationic ethyl amine (product) it can be seen that the product is more stable (-125.6 kJ/mol and -129.3 kJ/mol in MP2 and B3LYP methods, respectively) than the transition state.

3.2.4. Potential energy surface of cation–neutral reaction. The detailed potential energy surface of the cation–neutral reaction with all four possible reaction pathways is shown in Figure 3. Based on the stabilization energy of the reactants compared to the transition state of the cation–neutral reaction, the four possible reactions are placed in such a way that the reactant system having the highest stability

occupies the top position. In the potential energy surface, the abbreviations ‘OPT’ means that the cation is fully optimized and the acronym ‘SP’ that the cation single point energy is calculated at the optimized geometry of its neutral molecule. For the four reactions, it can be seen that the transition state of the cation–neutral reaction is more stable than the reactants. As a result all four reaction paths can be treated as barrierless and hence spontaneous. The reactant single point energies (SP) are higher relative to the transition state than when the cation is fully optimized (OPT). This can be easily explained as the fully optimized cation of the reactant will be lower in energy (more stable) than the single point energy of the cation at its neutral optimized geometry. Another important observation is that the product is lower in energy (more stable) than the transition state and the reactants for each reaction possible pathway. It is clear that all four possible reaction pathways are highly exothermic in nature. Based on the reactant that undergoes the ionization, the four reactions can be separated into two types, (1) where the ionized ammonia cation radical reacts with the neutral ethylene and (2) where the ionized ethylene cation radical reacts with the neutral ammonia and these are discussed below. As the reactions are barrierless, only the reactant and product energetics are compared.

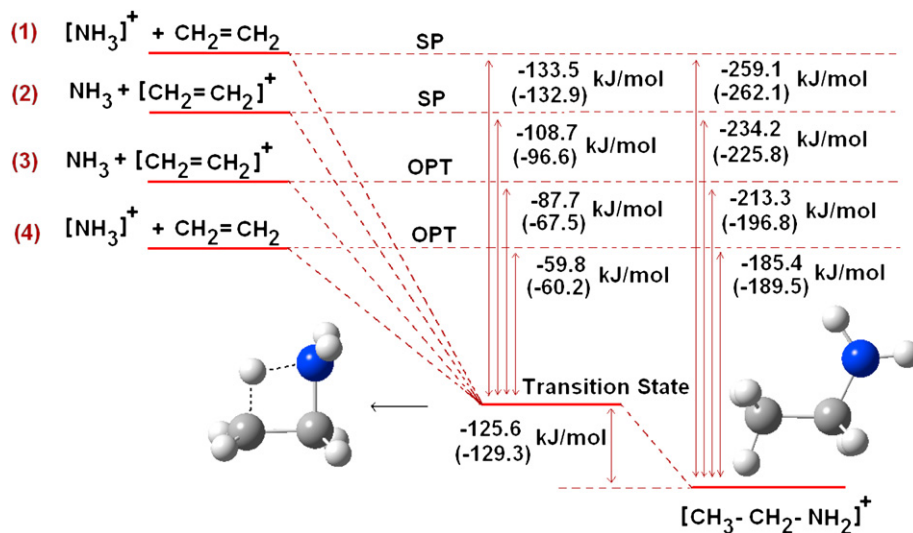


Figure 3. Potential energy surface of the cation–neutral hydroamination reaction. The ZPE corrected energy values are represented in kJ/mol for MP2 and B3LYP methodologies (B3LYP values are inside the bracket).

Case-1, where the ammonia is ionized to produce the $[\text{NH}_3]^+$ cation radical and this subsequently reacts with the neutral ethylene. If the cation relaxation time is slower than the reaction time, then the cation might undergo a structural relaxation before the reaction and if the relaxation of the cation is a slow process, then the generated cation of ammonia will immediately react with the neutral ethylene. Here both the situations are modelled by considering the fully optimized geometry of the cation for the former situation and the single point calculation for the cation at the optimized geometry of its neutral molecule for the latter situation. These two possibilities can be identified as paths (1) and (4), in Figure 3.

Case-2, where the ethylene is ionized to produce the $[\text{CH}_2=\text{CH}_2]^+$ cation radical and this subsequently reacts with the neutral ammonia. Similar to case-1, if the cation relaxation time is less than the reaction time, then the ethylene cation will undergo a structural relaxation before the reaction occurs and if the relaxation time of the cation is greater than the reaction time, then the generated cation of ammonia will immediately react with the neutral ammonia. Here both the situations are modelled by considering the fully optimized geometry of the cation of ethylene for the former situation and the single point calculation for the cation

at the optimized geometry of its neutral ethylene for the latter situation. These two possibilities can be identified as paths (2) and (3), in Figure 3. In both cases it can be seen that, when the reaction occurs through the unrelaxed geometry of the cation, the reaction is more exothermic than when it occurs through the relaxed geometry of the cation. Comparing MP2 data of paths (1) and (4), path (1) is 73 kJ/mol more exothermic than path (4). Similarly, comparing MP2 data of path (2) with (3), path (2) is 21 kJ/mol more exothermic than path (3). The difference between the relaxed and unrelaxed paths in case-1 is very high compared to case-2. This large difference in case-1 can be attributed to the large stabilization (lowering of the energy) of the ammonia cation radical after full minimization, as the geometry is relaxed from the pyramidal shape to the planar shape.

Comparing case-1 and case-2 it can be seen that, if the unrelaxed geometry of the cation is involved in reaction, then path (1), where the ammonia cation is involved is more exothermic than path (2), where the ethylene cation is involved in the reaction. The situation is reversed when the relaxed cation geometry is involved in the reaction. In other words, when the relaxed geometry of the cation is involved in the reaction, then path (3), where the ethylene

cation is involved is more exothermic than path (4), where the ammonia cation is involved in the reaction. As explained in the work of Hamann et al., the reaction of the ethylene cation with the neutral ammonia is preferred over the reaction of the ammonia cation with neutral ethylene (more product is obtained if the ethylene is ionized than if the ammonia is ionized).¹⁵ In such a case, the more exothermic nature of path (3) over path (4) (former path is around 27 kJ/mol more exothermic than the latter one) will explain the preference of the ethylene cation reacting with the neutral ammonia over the ammonia cation reacting with the neutral ethylene, as observed in the experiment of Hamann et al.¹⁵ Thus it is likely that the generated cation undergoes structural relaxation before reacting with the neutral reactant.

4. Conclusions

In summary, we have carried out a computational study on the reaction paths of the neutral–neutral as well as cation–neutral direct hydroamination reaction, using MP2 and B3LYP methodologies. Our calculation for the neutral–neutral hydroamination reaction involving ethylene and ammonia shows that, although the

reaction is exothermic in nature, it is forbidden by a large energy barrier and large negative reaction entropy. Our B3LYP results agree well with the experimental ΔH , ΔG and ΔS values and at the same time estimate the barrier height to be 228.9 kJ/mol for the neutral–neutral reaction. Calculations of cation–neutral direct hydroamination show that the reaction is barrierless. Also the cation–neutral reaction shows that, if the unrelaxed geometry of the cation of either ammonia or ethylene is involved in the reaction, the reaction is more exothermic than if the relaxed geometry of either cation is involved in the reaction. The experimental results of Hamann et al. show that the reaction between the cation of the ethylene and the neutral ammonia is preferred over the reaction between the cation of ammonia and the neutral ethylene.¹⁵ Our calculations show that, when the structurally relaxed ethylene cation reacts with the neutral ammonia, the process is more exothermic than when the relaxed ammonia cation reacts with the neutral ethylene and vice versa for unrelaxed geometry. In other words, our calculations suggest that in the experimental work of Hamann et al.¹⁵ the generated cation undergoes a structural relaxation process before reacting with the other neutral reactant.

Acknowledgements

S.S. thanks Claude-Leon foundation of South Africa for the postdoctoral fellowship. This material is based on work supported by the National Research Foundation, South Africa. This publication was made possible (in part) by a grant from the Carnegie Corporation of New York. The statements made and views expressed are, however, solely the responsibility of the author.

References and notes

- Pohlki, C.; Doye, S. *Chem. Soc. Rev.* **2003**, 32, 104.
- Muller, T. E.; Beller, M. *Chem. Rev.* **1998**, 98, 675.
- Weymouth, F. J.; Millidge, A. F. *Chem. Znd. (London)* **1966**, 887.
- Irick, G. *Acetic Acid and its Derivatives*. Chemical Industries Series; Dekker: New York, NY, 1993; Vol. 49, pp 27–33.
- Lloyd, D. L.; Eve, P. L.; Gammer, D. P. *Erdoel, Erdgas, Kohle* **1993**, 109, 266.
- Steinborn, D.; Taube, R. Z. *Chem.* **1986**, 26, 349.
- Taube, R. In *Applied Homogeneous Catalysis with Organometallic Compounds*; Cornils, B., Herrmann, W. A., Eds.; Wiley-VCH: Weinheim, 1996; Vol. 1, p 507.
- Heilen, G.; Mercker, H. J.; Frank, D.; Reck, R. A.; Jäckh, R. *Ullmann's Encyclopedia of Industrial Chemistry*, 5th ed.; VCH: Weinheim, 1985; Vol. A2, pp 1–36.
- Catalysis from A to Z*; Cornils, B., Herrmann, W. A., Schlogl, R., Wong, C.-H., Eds.; Wiley-VCH: Weinheim, 2000.
- Roundhill, D. M. *Chem. Rev.* **1992**, 92, 1.
- Benson, S. W. *Thermodynamical Kinetics: Methods for the Estimation of Thermodynamic Data and Rate Parameters*, 2nd ed.; John Wiley: New York, NY, 1976.
- Pedley, J. B.; Naylor, R. D.; Kirby, S. P. *Thermochemical Data of Organic Compounds*, 2nd ed.; Chapman and Hall: London, 1986; Appendix Table 1.2.
- Gasc, M. B.; Lates, A.; Pene, J. J. *Tetrahedron* **1983**, 39, 703.
- Straub, T.; Haskel, A.; Neyroud, T. G.; Kapon, M.; Botoshansky, M.; Eisen, M. S. *Organometallics* **2001**, 20, 5017.
- Hamann, T.; Bohler, E.; Swiderek, P. *Angew. Chem., Int. Ed.* **2009**, 48, 4643.
- Frisch, M. J.; Trucks, G. W.; Schlegel, H. B.; Scuseria, G. E.; Robb, M. A.; Cheeseman, J. R.; Montgomery, J. A., Jr.; Vreven, T.; Kudin, K. N.; Burant, J. C.; Millam, J. M.; Iyengar, S. S.; Tomasi, J.; Barone, V.; Mennucci, B.; Cossi, M.; Scalmani, G.; Rega, N.; Petersson, G. A.; Nakatsuji, H.; Hada, M.; Ehara, M.; Toyota, K.; Fukuda, R.; Hasegawa, J.; Ishida, M.; Nakajima, T.; Honda, Y.; Kitao, O.; Nakai, H.; Klene, M.; Li, X.; Knox, J. E.; Hratchian, H. P.; Cross, J. B.; Adamo, C.; Jaramillo, J.; Gomperts, R.; Stratmann, R. E.; Yazyev, O.; Austin, A. J.; Cammi, R.; Pomelli, C.; Ochterski, J. W.; Ayala, P. Y.; Morokuma, K.; Voth, G. A.; Salvador, P.; Dannenberg, J. J.; Zakrzewski, V. G.; Dapprich, S.; Daniels, A. D.; Strain, M. C.; Farkas, O.; Malick, D. K.; Rabuck, A. D.; Raghavachari, K.; Foresman, J. B.; Ortiz, J. V.; Cui, Q.; Baboul, A. G.; Clifford, S.; Cioslowski, J.; Stefanov, B. B.; Liu, G.; Liashenko, A.; Piskorz, P.; Komaromi, I.; Martin, R. L.; Fox, D. J.; Keith, T.; Al-Laham, M. A.; Peng, C. Y.; Nanayakkara, A.; Challacombe, M.; Gill, P. M. W.; Johnson, B.; Chen, W.; Wong, M. W.; Gonzalez, C.; Pople, J. A. *Gaussian 03, Revision C.01*; Gaussian: Wallingford CT, 2004.
- Rauk, A. *Orbital Interaction Theory of Organic Chemistry*, 2nd ed.; John Wiley: New York, NY, 2001.
- Dopfer, O. *Chem. Phys.* **2002**, 283, 63.
- Lee, S. T.; Oka, T. *J. Chem. Phys.* **1991**, 94, 1698.
- Ion and Cluster Ion Spectroscopy and Structure*; Botschwina, P., in Maier, J. P., Eds.; Elsevier: Amsterdam, 1989; p 59.
- Kraemer, W. P.; Spirko, V. J. *Mol. Spectrosc.* **1992**, 153, 276.
- Leonard, C.; Carter, S.; Handy, N. C.; Knowles, P. J. *Mol. Phys.* **2001**, 99, 1335.
- Koppel, H.; Domcke, W.; Cederbaum, L. S.; von Niessen, W. *J. Chem. Phys.* **1978**, 69, 4252.
- Merer, A. J.; Schoonveld, L. *Can. J. Phys.* **1969**, 47, 1731.
- Toriyama, K.; Okazaki, M. *Appl. Magn. Reson.* **1996**, 11, 47.
- Toriyama, K.; Okazaki, M. *Acta Chem. Scand.* **1997**, 51, 167.